Bladder Cancer xx (2020) x–xx
DOI 10.3233/BLC-200340
IOS Press

Research Report

Synthesis, Characterization, and Biological Activity of Anthraquinone-Substituted Imidazolium Salts for the Treatment of Bladder Cancer

Michael L. Stromyer[a], David J. Weader[a,b], Uttam Satyal[b], Philip H. Abbosh[b,*] and Wiley J. Youngs[a,*]
[a]*The Department of Chemistry, The University of Akron, East Buchtel Commons, Akron, OH, USA*
[b]*Molecular Therapeutics Program, Fox Chase Cancer Center, Cottman Avenue, Philadelphia, PA, USA*

Received 2 June 2020
Accepted 26 August 2020
Pre-press 12 September 2020

Abstract.
BACKGROUND: Bladder cancer is one of the most common types of cancer diagnosed each year, and more than half of patients have non-muscle invasive bladder cancer (NMIBC). The standard of care for patients with high-grade NMIBC is Bacillus Calmette-Guerin (BCG). Unfortunately, multiple BCG shortages have limited access to this treatment. Available alternatives using intravesical administration of chemotherapy have some efficacy, but lack prospective validation and long-term outcomes. Development of novel intravesical therapies may provide more active alternatives to BCG for patients with high-grade NMIBC.
OBJECTIVE: To develop an optimal imidazolium salt for the intravesical treatment of NMIBC and determine preliminary *in vitro* activity of anthraquinone-substituted imidazolium salts.
METHODS: The development of the anthraquinone-substituted imidazolium salts was undertaken in an attempt to increase the potency of this class of compounds by incorporating the quinone functional group observed in the chemotherapeutics doxorubicin, valrubicin, and mitomycin. All compounds were characterized by ^{1}H and ^{13}C NMR spectroscopy and infrared spectroscopy. Furthermore, these imidazolium salts were tested for *in vitro* cytotoxicity by the Developmental Therapeutics Program (DTP) on the NCI-60 human tumor cell line screening. Additional *in vitro* testing was performed against diverse bladder cancer cell lines (RT112, TCCSUP, J82, and UMUC13) using CellTiter-Glo® assays and colony-forming assays.
RESULTS: The NCI-60 cell line screening indicated that compound **7** had the highest activity and was concluded to be the optimal compound for further study. Using CellTiter-Glo® assays on bladder cancer cell lines, 50% growth inhibitory concentration (IC_{50}) values were determined to range from 32–50 μM after an exposure of 1 h, for compound **7**. Further evaluation of the compound by colony-forming assays showed the complete inhibition of growth at 10 days post a 100 μM dose of compound **7** for 1 h.

*Correspondence to: Wiley J. Youngs, Ph.D., Department of Chemistry, The University of Akron, 190 East Buctel Commons Akron, OH 44325, USA. Tel.: +1 330 972 5362; E-mail: youngs@uakron.edu. and Philip H. Abbosh, MD Ph.D., Molecular Therapeutics Program, Fox Chase Cancer Center, 333 Cottman Avenue Philadelphia, PA 19111, USA. Tel.: +1 215 214 4295; E-mail: Philip.Abbosh@fccc.edu.

ISSN 2352-3727/20/$35.00 © 2020 – IOS Press and the authors. All rights reserved
This article is published online with Open Access and distributed under the terms of the Creative Commons Attribution Non-Commercial License (CC BY-NC 4.0).

Uncorrected Author Proof

CONCLUSIONS: The most active lipophilic anthraquinone imidazolium salt, compound **7**, could be a viable treatment for non-muscle invasive bladder cancer as it exhibits a cell-killing effect at a 1 h time period and completely inhibits cancer regrowth in colony-forming assays.

Keywords: Anticancer, antitumor, anthraquinone, imidazolium salts, non-muscle invasive bladder cancer

Uncorrected Author Proof

INTRODUCTION

Bladder cancer is estimated to affect over 80,000 new patients nationally in 2020, with more than 17,000 deaths anticipated [1]. Additionally, bladder cancer is the 4th and 8th most prevalent cancer in men and women, respectively, with the most common stage at the time of diagnosis being non-muscle invasive bladder cancer (NMIBC) [2]. Many therapies are used for NMIBC, but few are effective at elimination of the disease in some patients. The current standard of care for NMIBC is intravesical treatment with Bacillus Calmette-Guerin (BCG). Although BCG is an effective therapy, it is currently underproduced, which puts many patients at risk for cancer recurrence, progression, and subsequent radical cystectomy [3, 4]. Immunotherapy isn't the only option as intravesical chemotherapy can be used as a treatment for NMIBC. A problem with intravesical chemotherapy is that the treatment has been shown to lead to 62% recurrence in intermediate grade patients within 5 years, according to a study performed by the European Association of Urology [5, 6]. This may be circumvented with a treatment regimen of gemcitabine/docetaxel that has shown a reduction of recurrence, but lacks the evaluation of long term outcomes and prospective validation [7]. Furthermore, there are more difficult cases to treat with high-grade NMIBC such as carcinoma *in situ* (CIS), which have shown cancer progression when treated with intravesical chemotherapy [8]. We presume that one of the reasons for the reduced efficacy of intravesical chemotherapy is that the activity of the chemotherapeutic used is dependent on prolonged exposure in order to be incorporated into the cell in S-phase (during DNA replication) or mitosis, when most chemotherapies exert their toxicity. Prolonged exposure requires longer intravesical retention of the chemotherapy to achieve a therapeutic effect, which is not practical for most patients.

Due to the numerous BCG shortages and the reduced efficacy of intravesical chemotherapy compared to BCG, novel chemotherapeutics are needed to treat bladder cancer. Development of novel anticancer materials is a necessity to combat bladder cancer and improve patient outcomes. We recently developed an imidazolium salt (**TPP1**) that selectively targets and is cytotoxic toward bladder cancer *in vivo* [9]. This compound has somewhat low potency, with 500–1000 μM concentrations needed to treat select bladder cancer models, although this is still easily achievable in an intravesical setting (for reference, gemcitabine is often given at a concentration of 2.00 g in 50.0 mL, or 152 mM). To increase the potency of imidazolium salts for the treatment of bladder cancer, quinone moieties (which are key functional groups in the highly cytotoxic chemotherapeutics doxorubicin, valrubicin, and mitomycin C (Fig. 1)) can be incorporated. Therefore, we present the synthesis and characterization of novel imidazolium salts containing anthraquinone moieties and their *in vitro* activity against bladder cancer.

MATERIALS AND METHODS

General considerations

All reactions were performed aerobically unless otherwise stated. Solvents and chemical reagents were unmodified and purchased from VWR, Fisher Scientific, or Sigma Aldrich. The synthesis of starting material **1** was performed by a modified literature procedure [10, 11]. ^{1}H and ^{13}C NMR spectra were acquired on an Inova 400 MHz instrument (^{13}C NMR 100 MHz). All NMR samples were prepared using DMSO-d_6 and spectra were referenced to DMSO-d_6 (^{1}H: 2.500 ppm, ^{13}C: 39.520 ppm). Infrared spectroscopy was performed on imidazolium salts **3**, **4**, **6**, and **7** using a Thermo Scientific iS5 FT-IR w/ iD7 attachment.

X-ray crystallographic analysis

Crystals of the compounds were coated in Paratone oil, mounted on a CryoLoop and placed on a goniometer under a stream of nitrogen. Crystal structure data sets were collected on a Bruker Kappa APEX II Duo CCD system equipped with a Mo I μ S

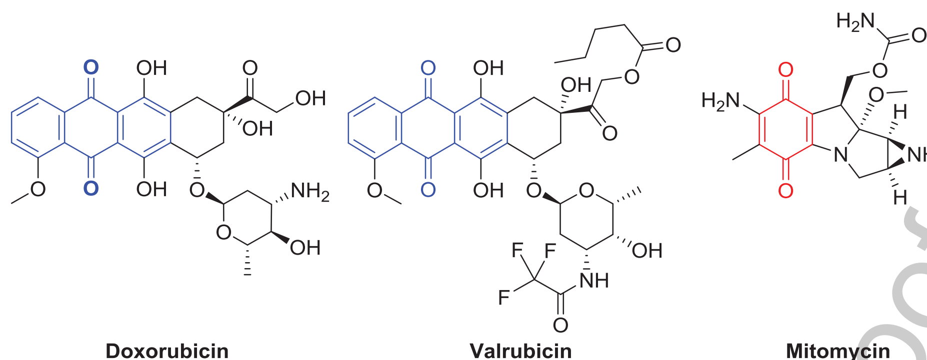

Fig. 1. Anthraquinone and quinone-containing chemotherapeutics, with anthraquinone (3-ring system) moieties highlighted in blue and quinone moieties (the basic functional group of a single conjugated cyclic dione) highlighted in red. Structures of doxorubicin, valrubicin, and mitomycin are shown.

source and a Cu I μ S micro-focus source equipped with QUAZAR optics ($\lambda = 1.54178$ Å). The unit cells were determined by using reflections from three different orientations. Data sets were collected using APEX II software packages. All data sets were processed using the APEX II software suite [12, 13]. The data sets were integrated using SAINT [14]. An empirical absorption correction and other corrections were applied to the data sets using multi-scan SADABS [15]. Structure solution, refinement, and modelling were accomplished by using the Bruker SHELXTL package [16]. The structures were determined by full-matrix least-squares refinement of F^2 and the selection of the appropriate atoms from the generated difference map. Hydrogen atom positions were calculated and $U_{iso}(H)$ values were fixed according to a riding model.

DTP NCI-60 cell line screening

The developmental therapeutics program (DTP) treatment protocol is summarized as follows: 60 cell lines ranging from leukemia to breast cancer are treated with a 10 μM concentration of the compound. The results are presented as growth percent. Continued growth is quantified from 0 to 100 and lethality is scored from –100 to 0. Further information on the experimental procedure for cell treatment can be viewed at NCI-DTP website (https://dtp.cancer.gov/discovery_development/nci-60/methodology.htm).

CellTiter-Glo® assay

Bladder cancer cell lines (RT112, TCCSUP, J82, and UMUC13) were seeded at 10,000 cells/well in black-walled 96 well plates and incubated for 24 h. Cells were treated with compound **7** in their respective media (as recommended by ATCC) at concentrations of 500 to 7.8 μM dissolved in two-fold dilution increments of vehicle for 1 h, followed by replacement of treatment media with normal growth media. After 24 h, plates with cells were incubated at room temperature for 30 min, followed by the addition of 20 μL of CellTiter-Glo® luminescent cell viability assay reagent (Promega) and mixing. After 2 min of incubation at room temperature, luminescence for each plate was measured using IVIS. Relative survival for each treatment group was calculated using vehicle control. All treatments were performed in quadruplicate.

Colony-forming assay

Cells were seeded at 500 cells/well in 6-well plates and 24 h later treated with 25 μM, 50 μM or 100 μM of compound **7** or vehicle for 1 h. Cells were then allowed to grow in normal media for 10 days followed by staining with crystal violet (0.5% crystal violet in 20% MeOH/water) and incubation at 4°C for 5 min. The wells were then washed several times with PBS and dried prior to imaging. All the experiments were performed in triplicate.

Synthesis of 2-(bromomethyl)-9,10-anthraquinone (1)

2-(Bromomethyl)-9,10-anthraquinone (compound **1**) was synthesized by a modified literature procedure [10, 11]. The radical initiator used was azobisisobutyronitrile (AIBN) instead of benzoyl peroxide (BPO). To obtain adequate purification for further

Uncorrected Author Proof

reactions the product was collected from the hot reaction mixture by vacuum filtration and subsequently recrystallized with ethanol.

Synthesis of 2-((imidazol-1-yl)methyl)-9,10-anthraquinone (2)

Imidazole (0.308 g, 4.52 mmol) was stirred at reflux in acetonitrile (10 mL) with potassium hydroxide (0.281 g, 5.01 mmol). After 15 minutes compound **1** (1.361 g, 4.52 mmol) was added and the reaction mixture was allowed to reflux for 24 h. The reaction was filtered hot to remove KBr and the filtrate volatiles were removed under reduced pressure. The resulting crude solid was stirred in hot water. The product was collected via vacuum filtration, washed with ethyl ether, and dried under vacuum. The solid was dissolved in dichloromethane and impurities were precipitated with ethyl ether. Upon filtration, the filtrate volatiles were removed affording compound **2** as a yellow solid (0.963 g, 73.9%). ^{1}H-NMR (400 MHz DMSO-d_6): δ 8.18 (m, 2H, Ar), 8.08 (d, 1H, Ar), 8.00 (s, 1H, Ar), 7.91 (dd, 2H, Ar), 7.83 (s, 1H, Ar), 7.72 (m, 1H, Ar), 7.26 (s, 1H, Ar), 6.96 (s, 1H, Ar), 5.45 (s, 2H, CH_2).

Synthesis of 1,3-bis((9,10-anthraquinone-2-yl) methyl)imidazolium bromide (3)

Compound **2** (0.499 g, 1.73 mmol) was refluxed in acetonitrile (8 mL) with compound **1** (0.535 g, 1.78 mmol) for 15 h. A yellow precipitate formed and was collected via vacuum filtration. The crude product was stirred in refluxing acetonitrile, collected via vacuum filtration and washed with THF and ethyl ether to produce compound **3** (0.609 g, 59.7%). ^{1}H-NMR (400 MHz DMSO-d_6): δ 9.61 (s, 1H, NCHN), 8.26 (d, 2H, Ar), 8.21 (m, 4H, Ar), 8.15 (m, 2H, Ar), 7.99 (s, 3H), 7.97 (m, 5H, Ar), 5.73 (s, 4H, CH_2). ^{13}C NMR (100 MHz DMSO-d_6): δ 181.9, 141.1, 137.2, 134.6, 134.5, 134.1, 133.3, 132.9, 132.8, 127.6, 126.7, 126.5, 123.3, 51.5. ATR-IR: 3068w (CH, sp^2), 3006w (CH, sp^2), 1674s (C = O), 1590m (C = C) cm^{-1}.

Crystal data for **3**: $C_{33}H_{21}BrN_2O_4$, M = 589.43, monoclinic, a = 11.5769(8) Å, b = 11.9943(8) Å, c = 36.529(2) Å, β = 98.832(4)°, V = 5012.2(6) Å^3, T = 100(2) K, space group C2/c, Z = 8, 21708 reflections measured, 5086 independent reflections (R_{int} = 0.0894). The final R1 values were 0.0594 (I > 2σ(I)). The final wR(F^2) values were 0.1074 (I > 2σ(I)). The final R1 values were 0.1276 (all data). The final wR(F^2) values were 0.1331 (all data).

Synthesis of 1-((9,10-anthraquinone-2-yl) methyl)-3-(naphthalen-2-ylmethyl)imidazolium bromide (4)

Compound **2** (0.283 g, 0.981 mmol) was refluxed in acetonitrile (2 mL) with 2-(bromomethyl)naphthalene (0.225 g, 1.02 mmol) for 15 h. A yellow precipitate formed and was collected via vacuum filtration (0.164 g, 32.8%). ^{1}H NMR (400 MHz DMSO-d_6) δ = 9.56 (1H, s, NCHN) 8.25 (4H, m, Ar) 7.98 (9H, m, Ar) 7.56 (3H, m, Ar) 5.71 (2H, s, CH_2) 5.65 (2H, s, CH_2). ^{13}C NMR (100 MHz DMSO-d_6): δ 182.0, 181.9, 141.2, 136.9, 134.63, 134.58, 134.1, 133.3, 132.9, 132.84, 132.82, 132.7, 132.6, 132.0, 128.8, 127.8, 127.7, 127.6, 127.5, 126.7, 126.6, 126.5, 125.7, 123.2, 123.0, 52.3, 51.4. ATR-IR: 3140w (CH, sp^2), 3009w (CH, sp^2), 2968w (CH, sp^3), 1672s (C = O), 1592 m (C = C) cm^{-1}.

Synthesis of 2-((benzimidazol-1-yl)methyl)-9,10-anthraquinone (5)

Benzimidazole (0.506 g, 4.52 mmol) was stirred at reflux in acetonitrile (10 mL) with potassium hydroxide (0.273 g, 5.01 mmol). After 30 minutes, **1** (1.271 g, 4.52 mmol) was added and the reaction mixture was allowed to reflux for 24 h. The reaction mixture was filtered hot to remove KBr and the filtrate volatiles were removed under reduced pressure. The resulting crude solid was stirred in hot water. Compound **5** was collected via vacuum filtration and washed with ethyl ether (0.520 g, 73.9%). ^{1}H-NMR (400 MHz; DMSO-d_6): δ 8.50 (s, 1H, Ar), 8.18 (m, 3H, Ar), 8.07 (s, 1H, Ar), 7.89 (m, 2H, Ar), 7.79 (d, 1H, Ar), 7.70 (m, 1H, Ar), 7.54 (m, 1H, Ar), 7.22 (m, 2H, Ar), 5.77 (s, 2H, CH_2).

Synthesis of 1,3-bis((9,10-anthraquinone-2-yl) methyl)benzimidazolium bromide (6)

Compound **5** (0.502, 1.73 mmol) was refluxed in acetonitrile (5 mL) with compound **1** (0.456 g, 1.78 mmol) for 16 h. A tan precipitate formed and was collected via vacuum filtration. The crude product was dissolved in DMF and precipitated with ethyl ether to afford compound **6** (0.752 g, 68.1%) ^{1}H-NMR (400 MHz DMSO-d_6): δ 9.61 (s, 1H, NCHN), 8.26 (d, 2H, Ar), 8.21 (m, 4H, Ar), 8.15 (m, 2H, Ar), 7.99 (s, 3H), 7.97–7.92 (m, 5H), 5.73 (s, 4H).

Uncorrected Author Proof

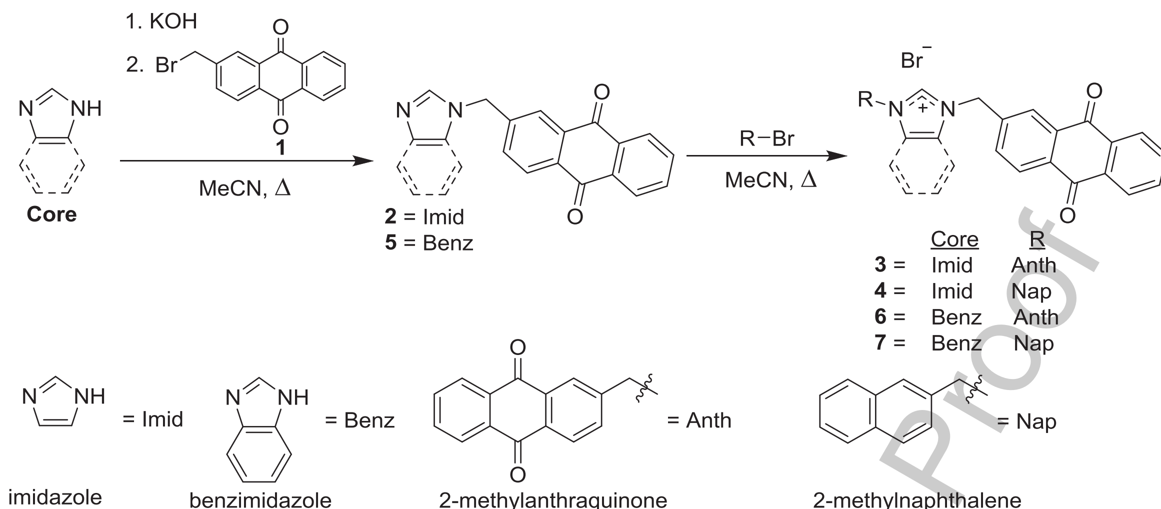

Scheme 1. Syntheses of compounds **2–7** by alkylation of imidazole or benzimidazole with **1** or 2-bromomethylnaphthalene.

^{13}C NMR (100 MHz DMSO-d$_6$): δ 182.0, 181.9, 143.7, 140.4, 134.6, 134.5, 134.0, 133.4, 132.9, 132.8, 131.1, 127.5, 127.1, 126.7, 126.5, 114.1, 49.6. ATR-IR: 3133w (CH, sp^2), 3071w (CH, sp^2), 3015w (CH, sp^2), 2928w (CH, sp^3), 1668s (C = O), 1603 m (C = C) cm^{-1}.

Synthesis of 1-((9,10-anthraquinone-2-yl) methyl)-3-(naphthalen-2-ylmethyl) benzimidazolium bromide (7)

Compound **5** (0.630, 1.86 mmol) was refluxed in acetonitrile (5 mL) with 2-(bromomethyl)naphtha lene (0.428 g, 1.94 mmol) for 16 h. A tan precipitate formed and was collected via vacuum filtration. The crude product was triturated with dichloromethane to afford an off-white solid, compound **7** (0.643 g, 61.7 %) ^{1}H-NMR (400 MHz DMSO-d$_6$): δ 10.24 (s, 1H, NCHN), 8.37 (s, 1H, Ar), 8.23 (m, 3H, Ar), 8.15 (s, 1H), 8.03 (dd, 4H, Ar), 7.94 (m, 4H, Ar), 7.66 (d, 3H, Ar), 7.57 (m, 2H, Ar), 6.10 (s, 2H, CH$_2$), 6.02 (s, 2H, CH$_2$). ^{13}C NMR (100 MHz DMSO-d$_6$): δ 182.5, 182.4, 143.8, 141.0, 135.06, 135.02, 134.4, 133.8, 133.3, 133.28, 133.24, 133.2, 133.1, 131.7, 131.6, 131.5, 129.2, 128.3, 128.2, 128.1, 127.9, 127.4, 127.3, 127.2, 127.1, 126.9, 126.2, 114.7, 114.4, 50.8, 50.0. ATR-IR: 3129w (CH, sp^2), 3069w (CH, sp^2), 3025w (CH, sp^2), 2952w (CH, sp^3), 1668s (C = O), 1591 m (C = C) cm^{-1}.

Crystal data for compound **7**: $C_{33}H_{23}BrN_2O_2$, M = 559.44, Triclinic, $a = 7.9808(4)$ Å, $b = 11.3358(5)$ Å, $c = 15.2282(8)$ Å, $\alpha = 74.908(3)^\circ$, $\beta = 86.015(3)^\circ$, $\gamma = 70.555(3)^\circ$ V = 5012.2(6) Å^3, T = 100(2) K, space group P-1, Z = 2, 20211 reflections measured, 5073 independent reflections ($R_{int} = 0.0640$). The final R1 values were 0.0601 ($I > 2\sigma(I)$). The final wR(F^2) values were 0.1359 ($I > 2\sigma(I)$). The final R1 values were 0.0854 (all data). The final wR(F^2) values were 0.1538 (all data).

RESULTS AND DISCUSSION

Synthesis and characterization

The syntheses of the anthraquinone-substituted imidazolium salt compounds **3, 4, 6,** and **7** are outlined in the general reactions of **Scheme 1**. Compounds **3** and **4** were first synthesized by deprotonation of imidazole with potassium hydroxide and then adding 2-(bromomethyl)anthracene-9,10-dione. The purified mono-substituted imidazole (compound **2**) was subsequently combined with either 2-(bromomethyl)anthracene-9,10-dione (compound **1**) or 2-(bromomethyl)naphthalene to form compounds **3** and **4** respectively. The compounds were first evaluated by ^{1}H NMR spectroscopy and the characteristic C^2 proton resonances were observed at 9.61 ppm for **3** and 9.57 ppm for **4**. Additionally a single resonance at 5.73 ppm was observed for the methylene protons of the symmetric compound **3**. In contrast the asymmetric imidazolium salt (compound **4**) yielded the methylene resonances at 5.71 and 5.65 ppm. Further characterization by ^{13}C NMR spectroscopy yielded the C^2 carbon resonance at 141 ppm for both compounds. The inequivalent car-

Uncorrected Author Proof

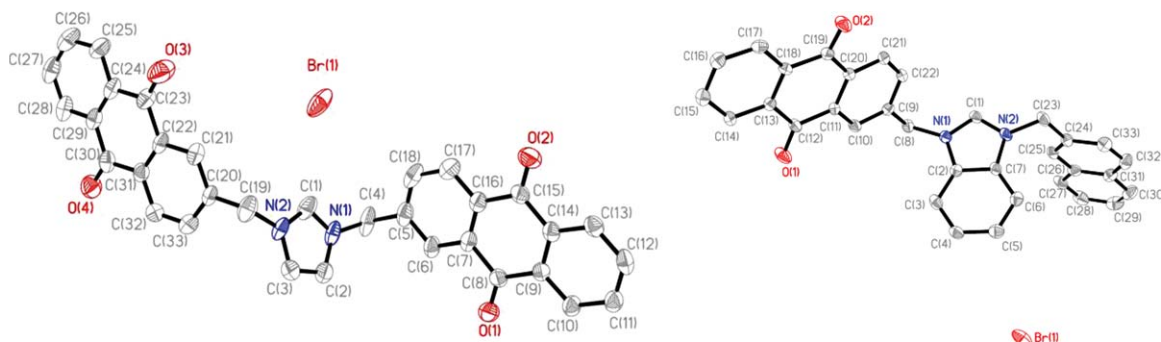

Fig. 2. Thermal ellipsoid plots of **4** and **7** with hydrogen atoms not shown for clarity. Thermal ellipsoids were drawn to 50% probability.

Table 1
One Dose NCI-60 Cell Line Screening for Compounds 3,4,6, and 7 (GI%)

Compound	Leukemia: CCRF-CEM	HL-60(TB)	K-562	MOLT-4	RPMI-8226	SR	NSCLC: A549/ATCC	EKVX	HOP-62	HOP-92	NCI-H226	NCI-H23	NCI-H322M	NCI-H460	NCI-H522
3	90.0	97.2	92.2	98.7	91.2	48.5	92.9	98.5	96.5	122.2	77.8	90.9	89.3	88.4	103.3
4	87.0	100.2	98.6	97.0	88.3	48.1	91.2	109.2	94.4	117.2	88.8	92.9	87.7	92.9	107.9
6	71.0	43.0	32.5	79.1	17.3	73.7	110.2	70.9	106.9	47.8	83.3	75.6	91.0	94.0	38.9
7	22.1	-49.2	17.6	28.1	2.5	38.1	91.0	73.9	76.2	15.6	63.9	56.5	75.4	63.4	34.1

Compound	Breast: MCF7	MDA-MB-231/ATCC	HS 578T	BT-549	T-47D	MDA-MB-468	CNS: SF-268	SF-295	SF-539	SNB-19	SNB-75	U251	Prostate: PC-3	DU-145
3	83.8	93.5	101.2	103.1	81.2	43.2	100.0	104.0	102.3	99.0	103.7	118.1	88.5	102.3
4	92.9	100.6	103.6	101.8	90.8	71.2	98.5	102.4	98.0	92.4	96.6	103.1	83.7	104.6
6	59.2	81.4	92.6	60.1	70.1	-32.2	72.5	94.9	84.1	79.5	62.8	85.8	38.8	114.6
7	39.9	26.2	62.2	47.0	41.2	-27.6	49.3	82.2	70.6	45.0	42.3	57.1	27.7	83.1

Compound	Colon: COLO 205	HCC-2998	HCT-116	HCT-15	HT29	KM12	SW-620	Renal: 786-0	A498	ACHN	CAKI-1	RXF 393	SN12C	TK-10	UO-31
3	97.7	100.3	92.2	99.9	89.3	80.4	85.0	64.7	140.2	108.3	97.3	104.8	102.6	136.8	83.9
4	104.0	99.2	89.0	97.8	91.9	88.1	92.2	99.4	107.7	104.1	95.3	110.5	101.8	130.4	84.0
6	58.6	79.1	84.3	98.1	73.1	77.8	84.2	98.8	98.3	108.4	96.5	N/A	74.4	107.3	82.5
7	24.4	46.2	41.2	89.8	51.5	25.5	64.4	61.2	77.9	92.4	40.5	62.6	47.8	67.8	72.8

Compound	Renal: 786-0	A498	ACHN	CAKI-1	RXF 393	SN12C	TK-10	UO-31	Ovarian: IGROV1	OVCAR-3	OVCAR-4	OVCAR-5	OVCAR-8	NCI/ADR-RES	SK-OV-3
3	64.7	140.2	108.3	97.3	104.8	102.6	136.8	83.9	90.2	88.8	98.8	102.5	97.2	103.5	98.2
4	99.4	107.7	104.1	95.3	110.5	101.8	130.4	84.0	91.7	94.1	93.8	100.6	100.9	97.4	102.7
6	98.8	98.3	108.4	96.5	N/A	74.4	107.3	82.5	29.6	40.8	58.7	84.6	89.5	104.4	105.3
7	61.2	77.9	92.4	40.5	62.6	47.8	67.8	72.8	3.7	34.9	47.2	59.3	41.4	91.1	83.2

Compound	Melanoma: LOX IMVI	MALME-3M	M14	MDA-MB-435	SK-MEL-2	SK-MEL-28	SK-MEL-5	UACC-257	UACC-62	Mean Growth
3	97.5	100.9	96.0	101.7	109.9	112.0	104.0	103.6	109.5	97.0
4	98.0	92.3	91.5	98.7	104.2	105.3	102.6	99.4	106.5	96.9
6	94.9	66.5	N/A	84.8	89.1	94.5	68.3	56.1	61.1	75.0
7	52.0	48.0	38.7	38.4	51.2	45.4	34.1	42.9	4.9	47.3

bonyl resonances of the 9,10-anthraquinone moieties were also observed for both compounds at 181.9 and 182.0 ppm.

The anthraquinone benzimidazolium salts, compounds **6** and **7,** were synthesized by a similar route to **3** and **4**, with formation of the mono-substituted benzimidazole (**5**) first, then a subsequent alkylation. Structure elucidation of both compounds was determined by ^{1}H NMR spectroscopy with the methylene resonances at 6.11 ppm for the symmetric compound **6** and 6.10 and 6.02 ppm for the asymmetric benzimidazolium salt, **7**. Furthermore the C^2 proton resonances were observed downfield at 10.26 and 10.24 ppm for **6** and **7** respectively. Similar to the ^{13}C spectra of compounds **3** and **4**, both **6** and **7** had C^2 carbon resonances at 143 ppm and the inequivalent anthraquinone carbonyl resonances at 182.0 and 181.9 ppm.

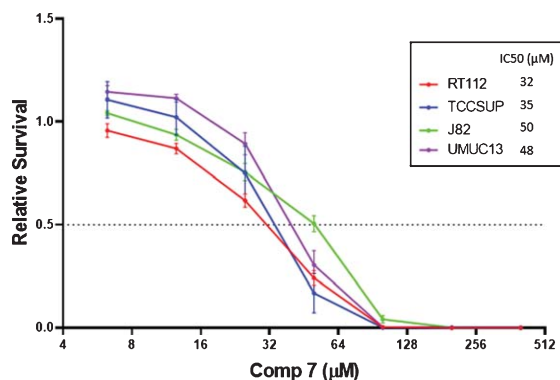

Fig. 3. IC_{50} values determined by the CellTiter-Glo® assay for a 1 h exposure of select bladder cancer cell lines to compound **7**.

To confirm the structures of the compounds discussed above, single crystal X-ray diffraction was used. Crystals suitable for analysis were obtained from vapor diffusion of ethyl ether into N,N-dimethylformamide solutions and only structures for compounds **4** and **7** were determined (Fig. 2).

In vitro biological evaluation of anthraquinone compounds as anticancer agents

The *in vitro* biological activity of compounds **3**, **4, 6,** and **7** was first evaluated by the Developmental Therapeutics Program (DTP) using the NCI-60 cell line screening (Table 1). At 10 μM the bisanthraquinone imidazolium salts, **3** and **6**, had little inherent activity toward most of the 60 cell lines with a 48 h exposure.

The asymmetric compounds **4** and **7** had increased activity in comparison to compounds **3** and **6** against the NCI-60 cell lines, with compound **7** exhibiting the most cytotoxicity at an average percent growth inhibition (GI%) of 47.3% over all cell lines. This potency is believed to be directly caused by the addition of the naphthalene substituent and increased lipophilicity of the benzimidazole, as similar activity

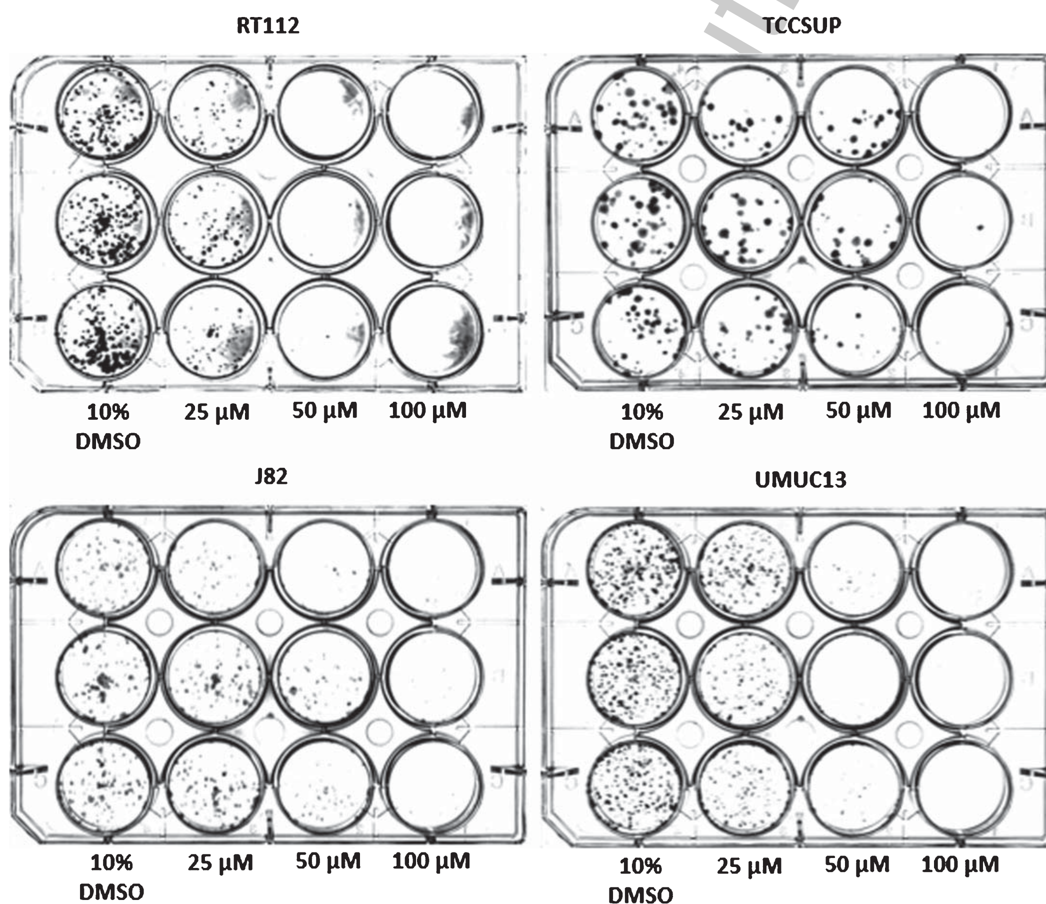

Fig. 4. Colony-forming assay of select bladder cancer cell lines 10 days after a 1 h treatment with compound **7**.

has been previously reported by the Youngs group with respect to lung cancer [17].

With preliminary data indicating the increased cytotoxicity of compound **7** against the NCI-60 cell line screening, further *in vitro* activity was evaluated against select bladder cancer cell lines. IC_{50} values of 32, 35, 50, and 48 μM were determined for a 1 h exposure of compound **7** to bladder cancer cell lines RT112, TCCSUP, J82, and UMUC13 respectively (Fig. 3). The shortened exposure time is necessary as intravesical treatments cannot be retained in patients for prolonged periods of time.

The long-term cytotoxicity of short-term exposure to compound **7** was evaluated next. Using the colony-forming assay, compound **7** was shown to inhibit cell growth against RT112 and UMUC13 at 50 μM (1 h exposure) after a recovery period of 10 days. When increasing the concentration to 100 μM, compound **7** inhibited cancer regrowth in all tested cell lines after 10 days recovery.

CONCLUSION

In this work, a series of anthraquinone-substituted imidazolium salts was synthesized. The bisanthraquinone imidazolium and benzimidazolium salts, when tested by DTP on the NCI-60 cell line screening, yielded little inherent activity against all cell lines at the 10 μM test concentration. Even though these compounds are lipophilic, the correlation between the naphthalene substituent and activity is apparent, as compounds **4** and **7** both exhibited activity against the cell lines in the screening. Moreover it was determined that replacement of the imidazole (**4**) with benzimidazole (**7**) resulted in a significant increase in cytotoxicity, believed to be due to the increase in lipophilicity. With preliminary data from the NCI-60 showing compound **7** to be the most cytotoxic of the compounds, it was chosen for further study. Compound **7** exhibited significant *in vitro* activity against select bladder cancer cell lines after a 1 h exposure time. Further, compound **7** prevented bladder cancer regrowth in the colony-forming assay against all tested cell lines over a period of 10 days. With these results compound **7** exhibits a cell-killing effect in an acceptable time period against bladder cancer cell lines and may be a highly effective treatment for NMIBC.

SUPPLEMENTARY INFORMATION

One dose NCI-60 human tumor cell line screening data for compounds **3**, **4**, **6**, and **7** as presented from DTP. NMR spectroscopy data for compounds **2–7**. IR spectroscopy data for compounds **3**, **4**, **6**, and **7**

Crystallographic Information File for **4** (CCDC # 1988214) and **7** (CCDC # 1988213) can be found free of charge on the Cambridge Crystallographic Data Center website.

ACKNOWLEDGMENTS

The authors would like to thank NCI's DTP for performing the 60 human tumor cell line screening with their one dose assay for compounds **3**, **4**, **5**, and **7**. We are also grateful for the funding provided by the University of Akron's Chemistry Department for the purchase of chemical reagents.

FUNDING

This work was funded by the following: PHA-BCAN Young Investigator Award, US-Avery Postdoctoral Fellowship, and the Fox Chase Center Core Grant (P30 CA006927). Additional funding for instrumentation was provided by the National Science Foundation (NSF) for NMR spectrometers (Nos. CHE-0341701 and DMR-0414599) and the X-ray diffractometer (CHE-0840446) used in this work. Also supported by Fox Chase Cancer Center Core grant P30 CA006927.

AUTHOR CONTRIBUTIONS

Conceptualization, M.S. and W.Y.; development and structural characterization, M.S.; biological investigation, D.W., U.S., and P.A.; writing-original draft preparation, M.S.; writing-review and editing, M.S., D.W., U.S., P.A., and W.Y. All authors have read and agreed to the published version of the manuscript.

CONFLICTS OF INTEREST

The authors declare no conflict of interest.

REFERENCES

[1] Cancer Facts & Figures 2020. Am Cancer Soc. 2020.
[2] Anastasiadis A, de Reijke TM. Best practice in the treatment of nonmuscle invasive bladder cancer. Ther Adv Urol. 2012;4:13-32.

Uncorrected Author Proof

[3] du Preez K, Seddon JA, Schaaf HS, Hesseling AC, Starke JR, Osman M, Lombard CJ, Solomons R. Global shortages of BCG vaccine and tuberculous meningitis in children. Lancet Glob Heal. 2019;7:e28-e29.

[4] Messing EM. The BCG Shortage. Bl. cancer (Amsterdam, Netherlands). 2017;3:227-28.

[5] Porten SP, Leapman MS, Greene KL. Intravesical chemotherapy in non-muscle-invasive bladder cancer. Indian J Urol. 2015;31:297-303.

[6] Kamat AM, Lamm DL. Current trends in intravesical therapy for bladder cancer. Contemp Urol. 2000;55:161-8.

[7] Steinberg RL, Thomas LJ, O'Donnell MA, Nepple KG. Sequential Intravesical Gemcitabine and Docetaxel for the Salvage Treatment of Non-Muscle Invasive Bladder Cancer. Bl. cancer (Amsterdam, Netherlands). 2015;1:65-72.

[8] van Rhijn BWG, Burger M, Lotan Y, Solsona E, Stief CG, Sylvester RJ, Witjes JA, Zlotta, AR. Recurrence and Progression of Disease in Non-Muscle-Invasive Bladder Cancer: From Epidemiology to Treatment Strategy. Eur Urol. 2009;56:430-42.

[9] Stromyer ML, Southerland MR, Satyal U, Sikder RK, Weader DJ, Baughman JA, Youngs WJ, Abbosh PH. Synthesis, characterization, and biological activity of a triphenylphosphonium-containing imidazolium salt against select bladder cancer cell lines. Eur J Med Chem. 2020;185: 111832.

[10] Zheng Y, Zhu L, Fan L, Zhao W, Wang J, Hao X, Zhu Y, Hu X, Yuan Y, Shao J, Wang W. Synthesis, SAR and pharmacological characterization of novel anthraquinone cation compounds as potential anticancer agents. Eur J Med Chem. 2017;125:902-13.

[11] Ellis LT, Perkins DF, Turner P, Hambley TW. The preparation and characterisation of cyclam/anthraquinone macrocyle/intercalator complexes and their interactions with DNA. J Chem Soc Dalt Trans. 2003;3:2728-36.

[12] Bruker SMART (Version 5.625). Madison, Wisconsin, USA: Buker AXS inc.; 2012.

[13] Bruker APEX II. Madison, Wisconsin, USA: Bruker ACS Inc.; 2012.

[14] Bruker SAINT. Madison, Wisconsin, USA. Bruker ACS Inc.; 2012.

[15] Bruker SADABS. Madison, Wisconsin, USA: Bruker AXS Inc.; 2012.

[16] Sheldrick GM. Crystal structure refinement with SHELXL. ACTA Crystallogr C. 2015;71:3-8.

[17] Wright BD, Deblock MC, Wagers PO, Duah E, Robishaw NK, Shelton KL, Southerland MR, DeBord MA, Kersten KM, McDonald LJ, Stiel Ja, Panzner MJ, Tessier Ca, Paruchuri S, Youngs WJ. Anti-tumor activity of lipophilic imidazolium salts on select NSCLC cell lines. Med Chem Res. 2015;24:2838-61.

Uncorrected Author Proof